DOI 10.24425/aee.2025.153908

Non-oriented electrical steel under bending and annealing effects

MOHAMED AMINE HEBRI[1], GRÉGORY BAUW[1], JEAN-PHILIPPE LECOINTE[1]✉, STÉPHANE DUCHESNE[1], SARA FAWAZ[1,2], GIANLUCA ZITO[3], IDIR ARSLANE[4], ABDENOUR ABDELLI[3], ADRIEN MAIER[5], CLÉMENT VANDEGINEN[4]

[1] *Université d'Artois, UR 4025, Laboratoire Systèmes Electrotechniques et Environnement Béthune, F-62400, France*

[2] *ESME, ESME Research Lab, Campus de Lille F-59000 Lille, France*

[3] *IFP Energies Nouvelles Rueil-Malmaison, 92852, France*

[4] *CRITT M2A Bruay-la-Buissière, 62700, France*

[5] *EREM - Etudes Réalisations et Maintenance Wavignies, F-60130, France*

e-mail: mohamedaminehebri@gmail.com, {gregory.bauw/✉ jphilippe.lecointe/stephane.duchesne/sara.fawaz}@univ-artois.fr, {gianluca.zito/abdenour.abdelli}@ifpen.fr, adrien.maier@erem.fr, {cvandingenen/iarslane}@crittm2a.com

(Received: 30.09.2024, revised: 11.05.2025)

Abstract: This study investigates the impact of bending stress and annealing on the magnetic performance of 3% silicon-iron non-oriented electrical steel (NOES). Samples were bent into diameters of 120 mm, 160 mm, and 200 mm representing the internal, average and external diameters of an axial flux machine and their magnetic properties, including permeability and iron losses, were measured. The results show that bending stress significantly degrades these properties, with smaller diameters causing greater deterioration. Annealing treatments were applied to restore performance, with partial or full recovery depending on the annealing temperature. A finite element (FE) model is proposed to account for the effects of bending on magnetic performance, incorporating three regions with distinct magnetic properties corresponding to different bending radii, using the commercial software JMAG-Designer. The study's findings provide valuable insights into the effects of bending and annealing on NOES, offering potential applications in toroidal transformers and axial flux machines.

Key words: annealing, bending stress, flux density, iron losses, non-grain-oriented silicon steel, permeability

1. Introduction

In the context of the fast development of electric vehicle technology, the aim is to improve powertrain efficiency to reduce the environmental impact of hybrid/electric vehicles [1]. The magnetic circuits of most electrical machines (motors or transformers) are made using silicon-iron electrical steels [2]. The various processes required to manufacture the magnetic circuits in the final machine degrade the initial performance of the magnetic materials. The most commonly studied processes in the literature are the cutting, punching, welding, shrink-fitting [3–6].

The design of the magnetic circuits of most common axial flux machines (generally double stator or double rotor machines with surface permanent magnets) requires one to roll-up the magnetic sheets using conventionally Non-Oriented Electrical Steel (NOES) [2]. However, NOES is not limited to these applications; it is also extensively used in other machine types, such as rotating electrical machines, including induction motors and synchronous machines. Although these radial flux machines do not involve the rolling-up of magnetic sheets, they can still take experience degradation of magnetic properties due to manufacturing processes such as cutting, punching, and assembly. The annealing strategies and numerical modeling approaches discussed in this study could also provide valuable insights for mitigating magnetic property degradations caused by such processes in these machines.

According to [7–10], rolling-up of magnetic laminations (applying bending stress) can change the alignment of magnetic domains, leading to a degradation of the permeability and an increase in the iron losses, depending on the rolling-up diameter and the magnetic material. This leads to higher iron and Joule losses, impacting efficiency and potentially the size of the magnetic circuit.

Annealing (heat treatment) can mitigate these effects by restoring the magnetic domains through recrystallization [11]. The grain size obtained during final annealing is one of the most important factors determining magnetic performance [12]. However, annealing benefits are balanced against its cost and time requirements.

This work addresses the challenge of quantifying NOES degradation as a function of bending radius, a common gap in the literature. In addition, it addresses the major problem of iron losses in axial flux machines due to sheet rolling. The study provides quantitative results, proposes a transformer model applicable to axial flux machines and demonstrates the impact of annealing on the restoration of magnetic properties.

In this article, we will study the effects of bending stress and annealing on NOES.

2. Presentation of analysis technique

To evaluate the bending effect, three toroids are made of 5 laminations of 0.2 mm thickness, forming a total thickness of 1 mm, and 30 mm width. They are equipped with a primary excitation winding and a secondary winding (B-coil), as shown in Fig. 1. The term "lap" refers to the overlap length used during the rolling process to ensure mechanical holding of the sample by the adhesive tape.

These diameters of 120, 160, and 200 mm were selected to correspond to the internal, average, and external diameters of the magnetic sheets in axial flux machines. These values were specifically chosen because they reflect the actual dimensions of a real axial flux machine. The samples were prepared entirely in the laboratory, where the magnetic sheets were manually rolled around a template to achieve the desired bending radii, and the primary and secondary windings were also manually added to complete the setup (Fig. 2).

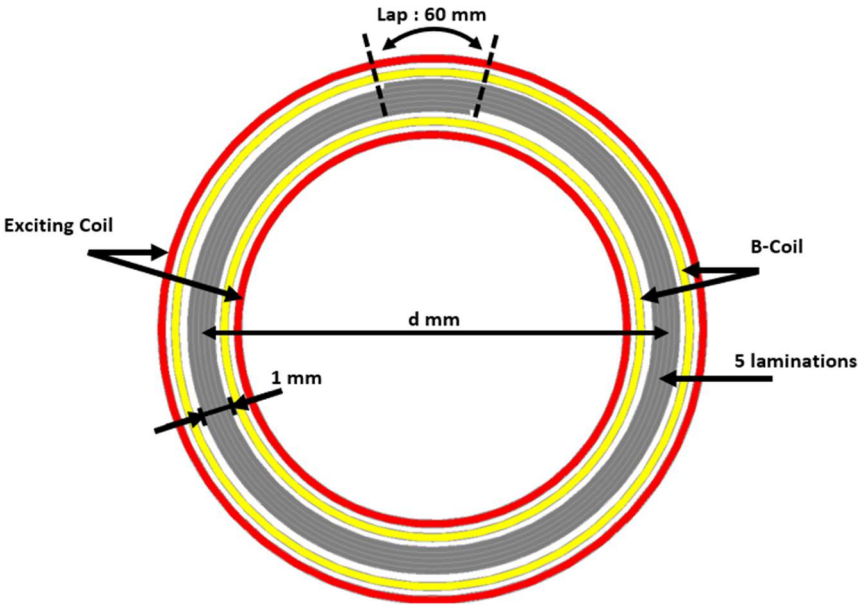

Fig. 1. Representation of wound sample for experimental analysis

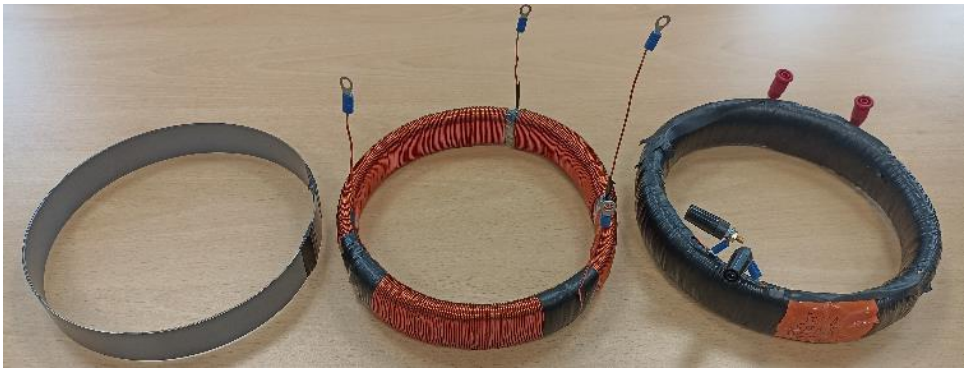

Fig. 2. Core manufacturing steps: torus alone, with the primary and secondary windings and final core

Comparison with the results obtained from an Epstein frame led us to ensure that the number of turns of the secondary winding is as close as possible to that of the primary winding. The number of primary and secondary turns for each torus are given in Table 1.

The Epstein frame used in this study is a standardized setup equipped with primary and secondary windings of 700 turns each (Fig. 3). The external dimensions of the core are 280×280 mm, with each arm of the frame is composed of 5 laminations connected with double overlap joints. A weight of 100 g is placed on each corner to minimize vibration effects. The dimensions of the individual laminations are 30×30 mm.

Table 1. number of primary and secondary turns for different bent samples

	d = 120 mm	d = 160 mm	d = 200 mm
Number of primary turns	381	418	461
Number of secondary turns	368	420	483

Fig. 3. Epstein frame for magnetic characterization

3. Measurement results

The B–H and iron losses curves for the different samples and degradation rates are shown in Figs. 4 and 5, respectively. The maximum relative permeabilities of the sheets, characterized with the Epstein frame and the torus of different dimensions are shown in Table 2. The reference is given by the annealed sheets characterized by Epstein frame. The degradation rate of the permeability (ratio_{μ_r}) and iron losses (ratio_P) are given by Eqs. 1 and 2 respectively.

$$\text{ratio}_{\mu_r}\,(\%) = \frac{H_{D(\text{mm})} - H_{\text{Epstein}}}{H_{\text{Epstein}}} \times 100, \tag{1}$$

where $H_{D(\text{mm})}$ represents the magnetic field intensity measured for a sample with a diameter of D, and H_{Epstein} corresponds to the value obtained using the standard Epstein method.

$$\text{ratio}_P\,(\%) = \frac{P_{D(\text{mm})} - P_{\text{Epstein}}}{P_{\text{Epstein}}} \times 100, \tag{2}$$

where $P_{D(\text{mm})}$ represents the iron losses measured for a sample with a diameter of D, and P_{Epstein} corresponds to the value obtained using the standard Epstein method.

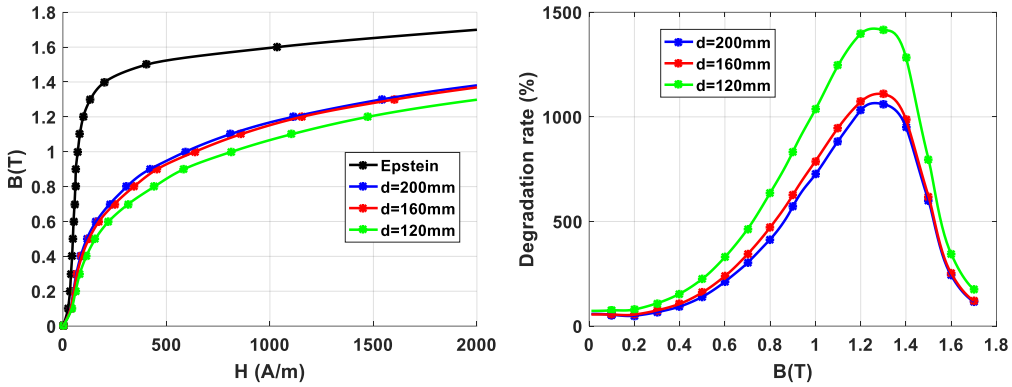

(a) (b)

Fig. 4. (a) B–H curves at 50 Hz; (b) permeability degradation rate

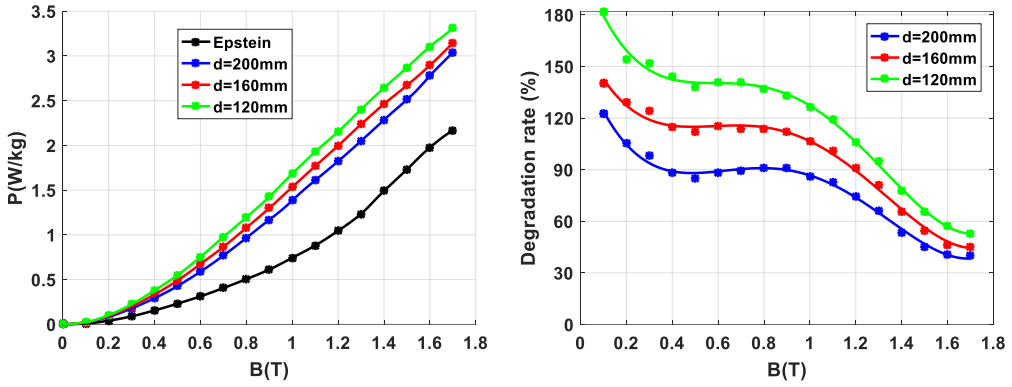

(a) (b)

Fig. 5. (a) Iron losses curves at 50 Hz; (b) degradation rate

Table 2. Maximum relative permeability of Epstein and bent samples

	Epstein samples	**Diameters of torus**		
		120 mm	**160 mm**	**200 mm**
Maximum relative permeability	11 440	2 932	3 527	3 734

Figure 4(b) shows the variation in the permeability degradation rate of the three toroids. A higher magnetic field is required to obtain a given flux density. As the toroid diameter decreases, the degradation increases. The variations of the degradation rates with B are similar for the three diameters, although the rates are different. The degradation rate is practically constant for flux density lower than 0.2 T. Between 0.2 T and 1.3 T, a very significant increase in the rate is observed. The maximum rates occur at the same flux density of 1.3 T for the 3 torus, corresponding to

the beginning of B–H curve knee of Epstein samples. Beyond this value, the degradation rate decreases significantly. For examples, magnetic fields of 2011 A/m, 1604 A/m, and 1540 A/m are respectively required to magnetize the 120 mm, 160 mm, and 200 mm torus at 1.30 T, compared with 132 A/m for Epstein strips, leading to the highest degradation rates of 1 415, 1 108 and 1 061% respectively. In addition, the maximum relative permeability varies from 11 440 to 2 932, 3 527 and 3 734 respectively.

Figure 5(b) shows also that the rolling up of the magnetic sheet affects the specific losses significantly. This increase evolves as a function of the winding diameters. For example, at an induction of 1.4 T, losses rise from 1.49 W/kg for the Epstein samples to 2.64 W/kg, 2.46 W/kg and 2.28 W/kg respectively for the 120, 160 and 200 mm toroids. The respective degradation rates are 77%, 65% and 53%. These degradation rate decreases almost linearly from 181%, 140% and 122% at 0.1 T to 57%, 48% and 42% at 1.7 T.

4. Annealing effect

Degradation due to rolling can be reduced by annealing. This allows magnetic domains to be rebuilt through recrystallization. The grain size obtained during final annealing is one of the most important factors determining magnetic performance. Despite its advantages, annealing is both expensive and time-consuming.

4.1. Experimental setup

To analyze the effect of annealing on the 3 toroids, a furnace from the manufacturer "Nabertherm" was used and shown in Fig. 6. Its peak temperature is 1 200°C.

Fig. 6. Annealing furnace (Nabertherm LH 216/12)

Each material requires a specific heat treatment, the parameters of which are: heating time, holding temperature and time, cooling time and atmosphere. The characteristics of a thermal annealing cycle are shown in Fig. 7.

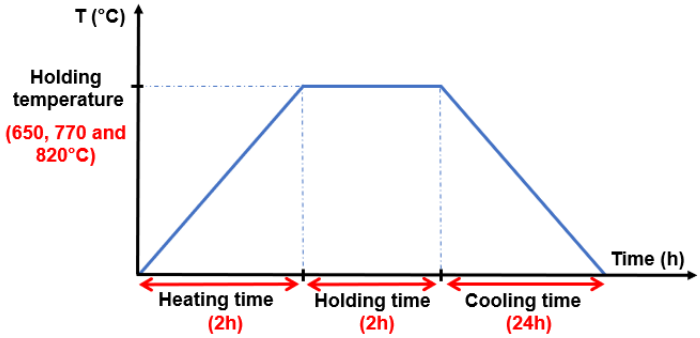

Fig. 7. Annealing characteristic

Figure 8 shows the support used for the mechanical holding of the toroids during the annealing process. This mica-based support can withstand temperatures up to 1 000°C, making it suitable for annealing.

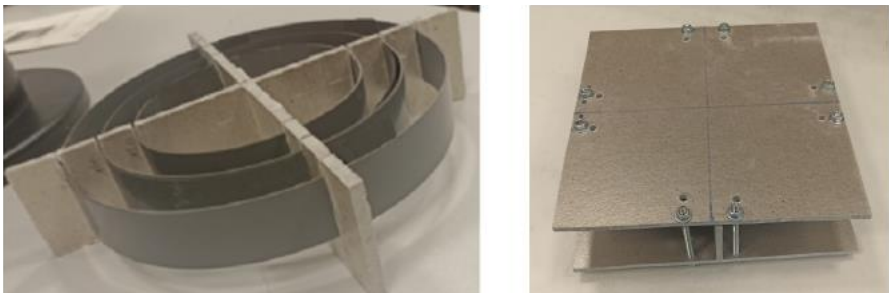

Fig. 8. Support used for holding the sheets during annealing

4.2. Annealing temperature impact on NO steel

According to the literature [9, 11, 13], the annealing temperature of FeSi materials, in general, varies between 600°C and 800°C. To this purpose, measurements to evaluate magnetic performance at different temperatures (650, 770, and 820°C) for a 200 mm sample were carried out to determine the most adapted temperature. The heating and holding times are set to 2 hours, while the cooling time is 24 hours. The heating and cooling times were determined by the furnace's ability to increase and decrease the temperature to reach the required maximum and ambient temperatures.

Figure 9 shows that increasing the temperature from 650 to 820°C leads to a better recovery of relative permeability and iron losses. For example, for a flux density of 1.5 T, the rate of permeability degradation is reduced from 225% to 20% when moving from a holding temperature

of 650°C to 820°C. A similar effect is observed for specific losses for the same induction, where the rate of degradation drops from 40% to 22%. For the rest of this study, we choose a holding temperature of 820°C for the NO sheet.

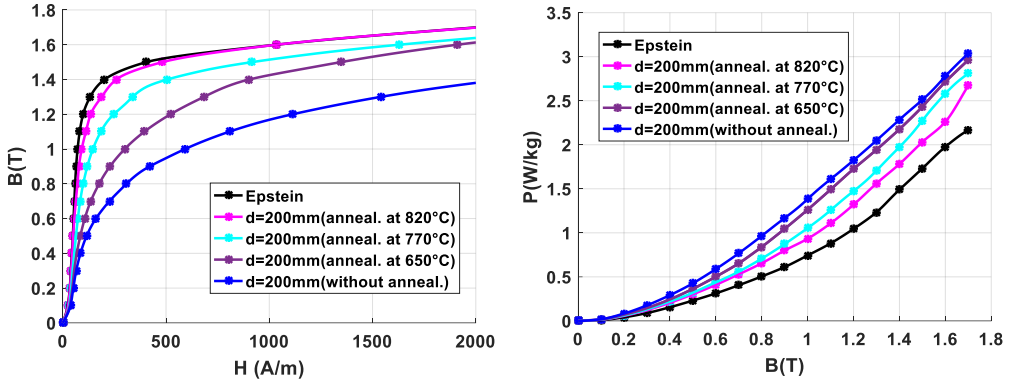

(a) (b)

Fig. 9. Annealing temperature impact at 50 Hz on: (a) B–H curves; (b) iron losses

4.3. Annealing on NO steel at 820°C

The number of primary and secondary turns for each torus after annealing are given in Table 3. Figure 10 shows the NO steel samples before and after annealing at 820°C.

Table 3. number of primary and secondary turns of different bent samples after annealing

	d = 120 mm	d = 160 mm	d = 200 mm
Number of primary turns	382	455	467
Number of secondary turns	394	451	452

Fig. 10. NO steel before and after annealing

We introduce the recovery rate ($\text{ratio}_{\text{recovery}}$), which represents the difference between the degradation rate before annealing ($\text{ratio}_{(\text{before anneal.})}$ and the degradation rate after annealing ($\text{ratio}_{(\text{after anneal.})}$). It is given by the following Eq. (3):

$$\text{ratio}_{\text{recovery}}\,(\%) = \frac{\text{ratio}_{(\text{before anneal.})} - \text{ratio}_{(\text{after anneal.})}}{\text{ratio}_{(\text{before anneal.})}} \times 100, \tag{3}$$

The B–H curve and specific losses of the NO sheet samples, their degradation and recovery rates following annealing, are presented in Figs. 11 and 12. The maximum relative permeabilities of different dimensions before and after annealing are given in Table 4.

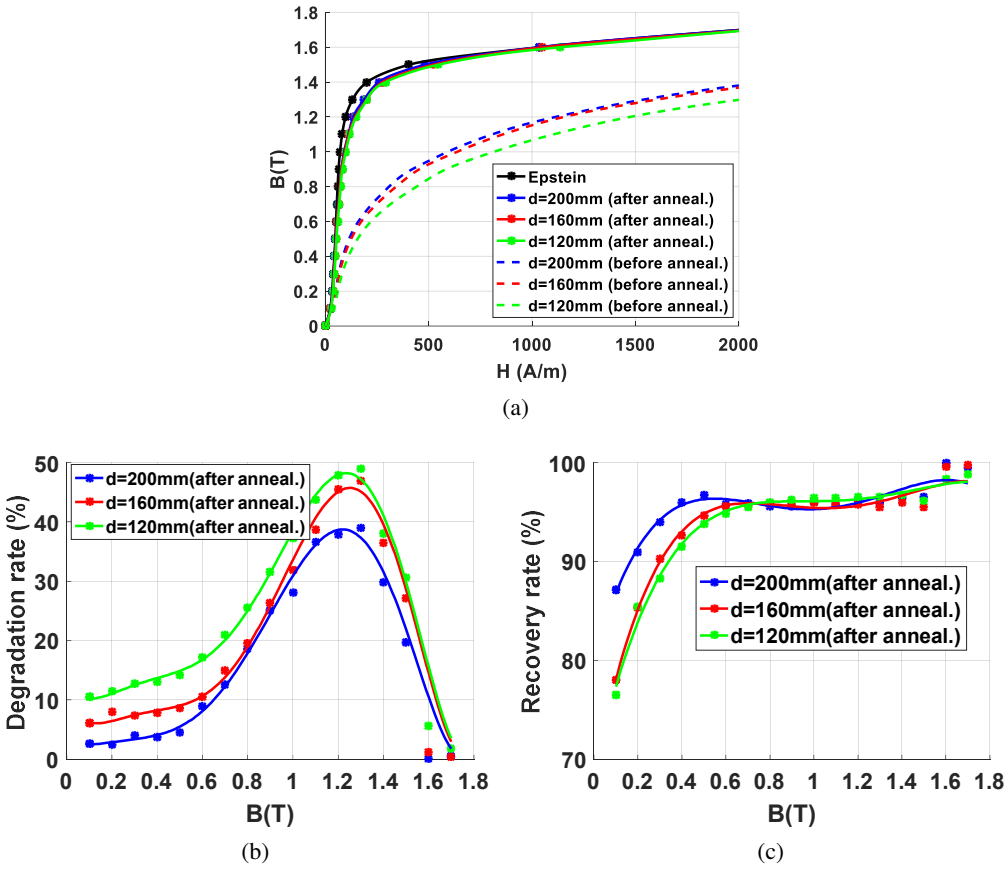

Fig. 11. Annealing impact at 820°C on: (a) B–H curves; (b) degradation rate; (c) recovery rate

Figure 11 shows that the annealing significantly improves the magnetic permeability of the three samples with different dimensions, with the three curves almost superimposed. However, all three toroids still show a certain rate of degradation compared to the healthy sheet, varying between 0 and 50%, in contrast to rates between 55 and 1 415% before annealing. After annealing, the toroid with the smallest diameter showed the highest rate of degradation compared with the

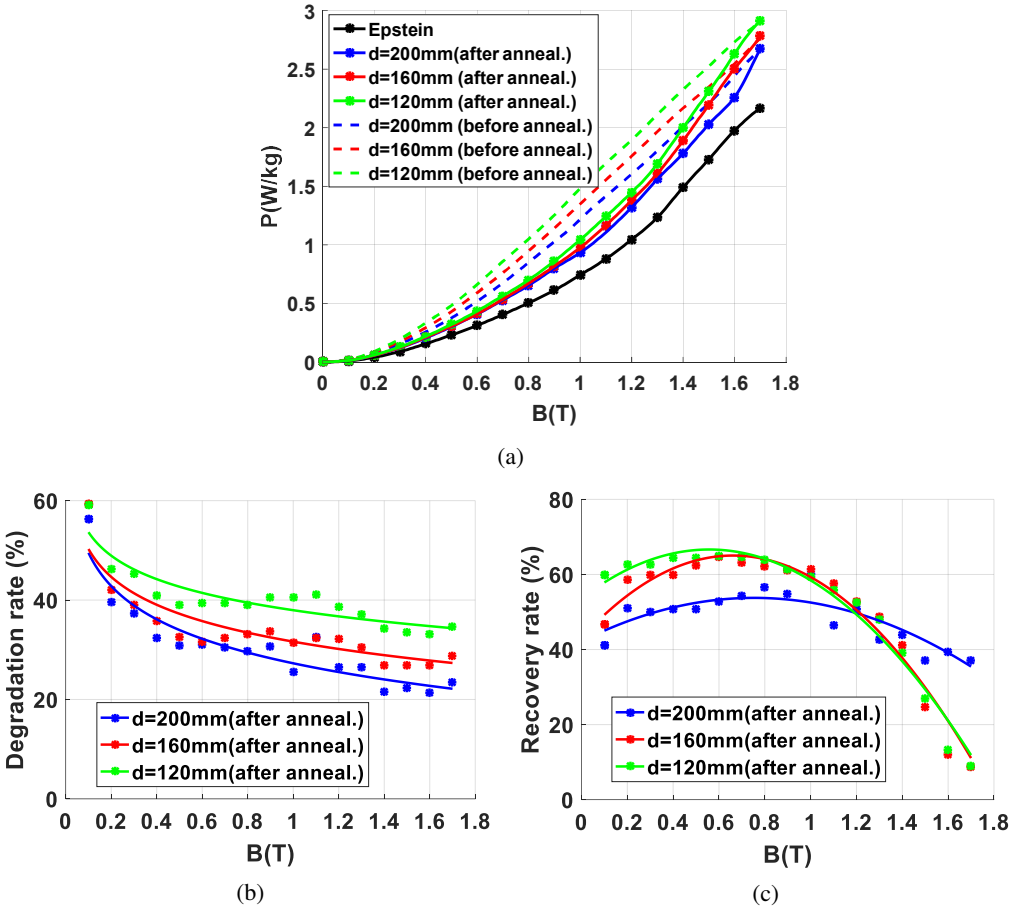

Fig. 12. Annealing impact at 820°C on: (a) iron losses; (b) degradation rate; (c) recovery rate

Table 4. Maximum relative permeability of bent samples before and after annealing

Maximal relative permeability	**Epstein samples**	**Diameters of torus**		
		120 mm	**160 mm**	**200 mm**
Before annealing	11 440	2 932	3 527	3 734
After annealing		8 696	9 059	9 140

larger diameters. There is a possibility that the smaller diameter degradation is influenced by strong bending stress and plastic deformation [8], or that the annealing process used is not well-suited for these smaller dimensions. Annealing resulted in strong permeability recovery, with rates ranging from 80 to 99% for all three samples, compared with performance before annealing. The recovery rates are practically superimposed for the three diameters analyzed. For example, after annealing, toroids with dimensions of 120 mm, 160 mm and 200 mm have maximum relative permeabilities of 8 696, 9 059 and 9 140 respectively, compared with 2 932, 3 527 and 3 734 before annealing.

Figure 12 shows that the annealing also improves the iron losses for all three samples. On the other hand, they still show a rate of degradation relative to the healthy sheet, which varies between 20 and 60, in contrast to the rates between 30 and 180% obtained before annealing. Annealing reduced iron losses, resulting in recovery rates ranging from 20 to 72% for all three samples. At high inductions (> 1.4 T), the recovery rate dropped sharply to values below 40% for all three samples.

We conclude that annealing toroids of different diameters in NO steel at 820°C in the absence of a controlled atmosphere results in very high-performance recovery in terms of permeability (up to 99%) and good recovery in terms of iron losses (up to a maximum value of 72%).

5. Numerical model

The properties have been integrated to a toroidal transformer in a FE model. This transformer is divided into three regions with different magnetic properties (B–H curves and specific losses). The diameter of the first region varies between 120 mm and 140 mm. This region takes the magnetic properties of the 120 mm diameter toroid analyzed previously. The magnetic properties of the second region are those of the 160 mm diameter toroid, with diameters between 140 and 180 mm. The diameter of the third region varies between 180 and 200 mm, this region has the magnetic properties of 200 mm diameter cores. Figure 13 shows the dimensions of analyzed model and the different regions.

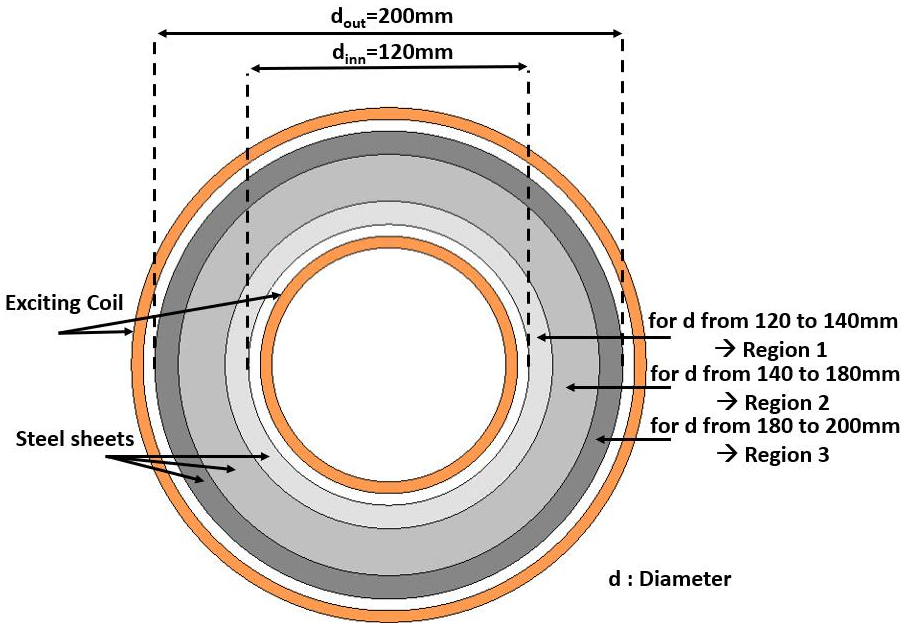

Fig. 13. Dimensions of the analyzed torus and application of degraded magnetic properties in different regions

A magnetic transient study at 50 Hz is carried out, with a sinusoidal current supply. The model has a depth of 30 mm (similar to an Epstein strip) and includes 100 turns. The mesh consists of 81 350 elements. A laminated factor of 0.96 was introduced in the software to account for its impact on magnetic performance, considering the effect of coating and the slight reduction in permeability caused by laminations. The numerical modeling is based on a finite element analysis (FEA) performed using the commercial software JMAG-Designer Ver.22.0, which enables the consideration of magnetic circuit saturation and harmonics. The calculation of iron losses is performed using the classical approximation of the Steinmetz model, which relies on standardized measurements. The simulations are carried out using an HP Z2 Mini G9 Workstation with a 12th Gen Intel®Core™i9-12900K @ 3.20 GHz (16 cores) and 64 GB RAM. The total simulation time is approximately 10 minutes. This approach was inspired by [8], where a conventional transformer with rounded corners was analyzed. In this study, the approach has been adapted and applied to a toroidal transformer or the yokes of an axial flux machine, focusing on the impact of bending and annealing on magnetic performance.

Figure 14 represents the flux density distribution at a maximum current of 1 A, for without bending stress, with bending stress before annealing and with bending stress after annealing sheet properties.

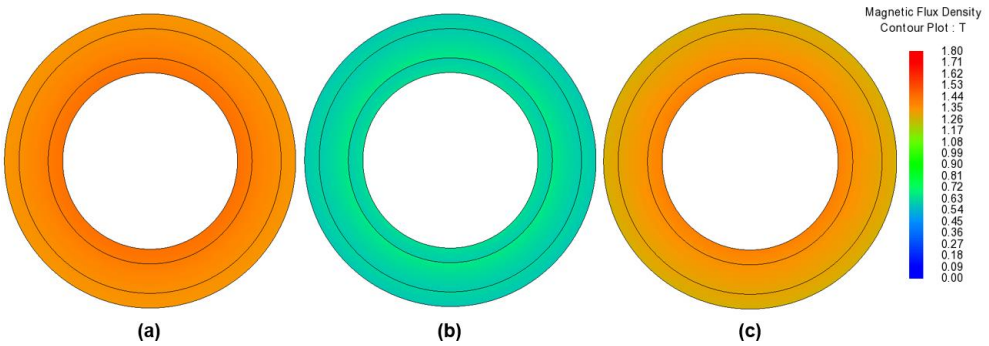

Fig. 14. Flux density distribution at 50 Hz and 1 A: (a) properties without bending stress; (b) properties with bending stress before annealing; (c) properties with bending stress afer annealing at 820°C.

In the case where the same current is applied, different levels of flux density are observed in the three cases studied:

– 1.40 T; properties without bending stress,
– 0.60 T; properties with bending stress before annealing,
– 1.35 T; properties with bending stress after annealing.

A comparison of the iron losses of the 3 different cases is relevant for the same average flux density. Table 5 shows the current required for the three cases studied above, and the corresponding level of losses, at 1.4 T and 50 Hz. Figure 15 shows the distribution of iron losses at 1.4 T for sheet steel properties in the three cases studied.

The difference in current between the two transformers with electrical steel data without bending stress (reference, Epstein data) and with bending stress before annealing is 7.5 A. This difference will have a significant impact on Joule losses, and therefore on efficiency. If the stressed electrical steels are annealed, the current difference decreases to 0.3 A.

Table 5. Values of flux density, excitation current and iron loss for: (a) without bending stress; (b) with bending stress before annealing; (c) with bending stress after annealing at 820°C

	(a): without bending stress	**(b):** with bending stress	**(c):** with bending stress after annealing
Average flux density (T)	1.40	1.40	1.40
Peak current (A)	1.00	8.50	1.30
Core Losses (W)	16.38	24.22	20.28

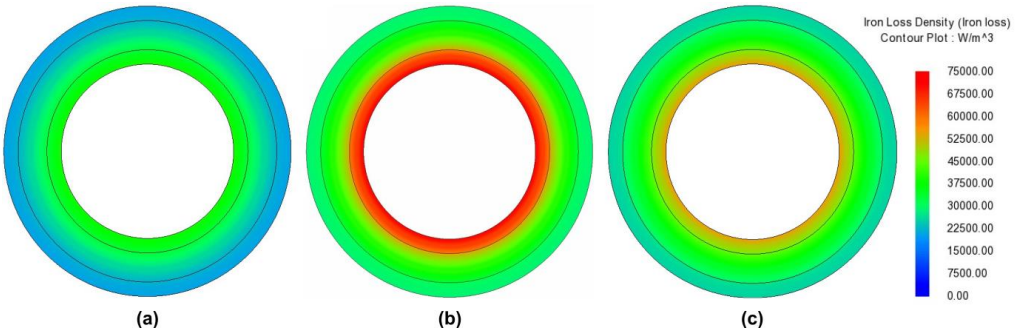

Fig. 15. Iron loss density distribution at 50 Hz and 1.4 T: (a) properties without bending stress; (b) properties with bending stress before annealing; (c) properties with bending stress afer annealing at 820°C

Iron losses are highest at the inner radius in all three cases Table 5 shows that iron losses at 1.4 T are lowest in the unstressed case (16.38 W) and highest in the case of bending stress (24.22 W). Annealing this toroid under bending stress and reduced stress reduced the losses to 20.80 W.

6. Conclusion

The bending stress deteriorates remarkably the magnetic properties of NOES, depending on the bend radius, the smaller the radius, the greater the deterioration in permeability and losses. By annealing the rolled-up NOES, a partial or total recovery of their magnetic performances can be achieved. Annealing is a complex process, and its efficiency depends on several parameters: holding time and temperature, heating and cooling time, and annealing atmosphere. In this work, we focused on holding temperature, as this was not supplied by the supplier. It figured out that a holding temperature of 820°C is better than 650°C and 770°C. Annealing at 820°C resulted in recoveries of 80 to 100% for permeability, and 20 to 70% for losses. Through the numerical model, we have seen the importance of annealing. In fact, to magnetize the transformer at 1.4 T, currents of 8.5 and 1.3 A are required for steels with bending stress before and after annealing respectively. These current values will have a direct impact on joule losses. In both cases, annealing reduced iron losses from 24.22 to 20.28 W, or 16%. Annealing improves permeability, thus reducing magnetizing current, and therefore Joule losses, as well as iron losses, which will have an impact on transformer efficiency. This numerical model can be applied to the stator or rotor yokes of axial flux.

In terms of practical Implications and Recommendations, the results of this study highlight critical ideas and practical recommendations for the design and manufacture of electrical machines, particularly axial flux machines and toroidal transformers.

- The research shows that bending stress during the manufacturing process significantly deteriorates the magnetic properties of NOES, leading to increased iron losses and reduced permeability. This highlights the importance of optimizing the bending radius to minimize such degradation. Where tight bends are unavoidable, it is recommended to incorporate annealing processes at a temperature to restore magnetic properties and reduce iron losses in order to improve overall performance. However, due to the high costs and time constraints of annealing, a cost-benefit analysis should guide its application in production workflows.
- Furthermore, if annealing is deemed too costly or impractical, alternative strategies could be considered. For example, segmented yokes with appropriate mechanical support could offer a viable solution for reducing bending stresses, although this approach introduces additional complexity into the mechanical assembly. Investigating different materials that are less sensitive to bending stresses could also attenuate performance degradation. In addition, further studies could focus on extending this methodology to analyze the impact of bending and annealing at variable frequencies, considering that real applications often operate at multiple frequency ranges (such as in the case of a dual-stator axial flux machine).
- The finite element model used in this study provides a valuable predictive tool for assessing the impact of bending and annealing on magnetic performance. It enables engineers and manufacturers to refine material modeling in simulations, leading to more accurate design optimizations and improved energy efficiency of electrical devices. The methodology can also be extended to different materials and operating conditions, making it a flexible approach to improving the performance of transformers and electrical machines.

Future research could explore the effects of varying annealing atmospheres, cooling rates, and their integration into advanced industrial workflows, such as those for electric vehicle powertrains, where efficiency and performance are paramount. By adopting these strategies, manufacturers can achieve better material utilization, reduce energy losses, and develop more efficient, high-performing machines for diverse applications. As a perspective, future work could also explore the impact of anisotropic properties in non-grain-oriented steel under bending conditions and investigate microstructural changes such as dislocation density, recrystallization, and grain growth to deepen the understanding of bending and annealing effects.

It is acknowledged that the use of only three diameters may limit the generalization of the findings to other geometries; however, the methodology proposed in this study can be extended in future work to include additional bending conditions and a broader range of dimensions, ensuring its applicability to diverse industrial scenarios.

References

[1] Auverlot D., Meilhan N., Mesqui B., Pommeret A., *Government Policy in Favour of Ultra-low Emission Vehicles* (in French), France Stratégie (2018), available online: https://www.strategie.gouv.fr/publications/politiques-publiques-faveur-vehicules-tres-faibles-emissions.

[2] Pyrhonen J., Jokinen T., Hrabovcova V., *Design of Rotating Electrical* Machines (Second Edition), Wiley (2014), DOI: 10.1002/9780470740095.

[3] Rebhaoui A., Randi S., Demian C., Lecointe J.-P., *Analysis of flux density and iron loss distributions in segmented magnetic circuits made with mixed electrical steel grades*, IEEE Transactions on Magnetics, vol. 58, no. 8, pp. 1–11 (2021), DOI: 10.1109/TMAG.2021.3138984.

[4] Messal O., Kedous-Lebouc A., Youmssi A., *Experimental evaluation of the punching impact on the dynamic magnetic performances of M330-35A SiFe steel*, European Journal of Electrical Engineering, vol. 18, no. 5–6, pp. 413–423 (2017), https://hal.science/hal-02278160/.

[5] Krings A., Nategh S., Wallmark O., Soulard J., *Influence of the Welding Process on the Performance of Slotless PM Motors with SiFe and NiFe Stator Laminations*, IEEE Transactions on Industry Applications, vol. 50, no. 1, pp. 296–306 (2014), DOI: 10.1109/TIA.2013.2270972.

[6] Takahashi N., Morimoto H., Yunoki Y., Miyagi D., *Effect of shrink fitting and cutting on iron loss of permanent magnet motor*, Journal of Magnetism and Magnetic Materials, vol. 320, no. 20, pp. 925–928 (2008), DOI: 10.1016/j.jmmm.2008.04.170.

[7] Wang Z., Li S., Wang X., Cui R., Zhang W., *Modeling of surface layer and strain gradient hardening effects on micro-bending of non-oriented silicon steel sheet*, Materials Science and Engineering: A, vol. 771, pp. 498–507 (2018), DOI: 10.1016/j.msea.2017.08.085.

[8] Hagihara H., Takahashi Y., Fujiwara K., Ishihara Y., Masuda T., *Magnetic properties evaluation of grain-oriented electrical steel sheets under bending stress*, IEEE Transactions on Magnetics, vol. 50, no. 1, pp. 1–4 (2014), DOI: 10.1109/TMAG.2013.2286626.

[9] Saito A., Yamamoto T., Iwasaki H., *Magnetization properties and domain structures of grain-oriented silicon steel sheets due to bending stress*, IEEE Transactions on Magnetics, vol. 36, no. 5, pp. 3078–3080 (2000), DOI: 10.1109/20.908686.

[10] Cossale M., Krings A., Soulard J., Boglietti A., Cavagnino A., *Practical investigations on cobalt-iron laminations for electrical machines*, IEEE Transactions on Industry Applications, vol. 51, no. 4, pp. 2933–2939 (2015), DOI: 10.1109/ICELMACH.2014.6960363.

[11] Cunha M.A., Paolinelli S.C., *Effect of the annealing temperature on the structure and magnetic properties of 3% Si non-oriented steel*, Journal of Magnetism and Magnetic Materials, vol. 254, pp. 379–381 (2003), DOI: 10.1016/S0304-8853(02)00912-5.

[12] Wang J., Li J., Mi X., Zhang S., Volinsky A.A., *Rapid annealing effects on microstructure, texture, and magnetic properties of non-oriented electrical steel*, Metals and Materials International, vol. 18, pp. 531–537 (2012), DOI: 10.1007/s12540-012-3024-0.

[13] Kestens L., Jacobs S., *Texture control during the manufacturing of nonoriented electrical steels*, Texture, Stress, and Microstructure, vol. 2008, pp. 1–9 (2008), DOI: 10.1155/2008/173083.